RSC Advances

PAPER

View Article Online
View Journal | View Issue

Cite this: *RSC Adv.*, 2025, **15**, 25436

An NMR insight into the solvatochromic behaviour of Brooker's merocyanine dyes†

Michal Afri,[a] Hugo E. Gottlieb,[a] Natalia Fridman[b] and Abed Saady *[a]

Received 28th May 2025
Accepted 9th July 2025

DOI: 10.1039/d5ra03758a

rsc.li/rsc-advances

Systematic NMR/UV-Vis analysis of Brooker's merocyanine dyes reveals solvent polarity governs electronic structure and spectroscopy. Absorption maxima ^{13}C and ^{15}N NMR shifts correlate with $E_T(30)$, probing zwitterionic/vinylogous amide. Substituent and solvent effects modulate these interactions, directly linking colour changes to electronic structure for rational design of environment-sensitive probes.

Introduction

Nuclear magnetic resonance (NMR) spectroscopy is a fundamental tool for probing the structure, dynamics, and interactions of organic molecules, providing detailed insights that are indispensable in material science, drug development, and biochemical research.[1–3] NMR enables chemists to elucidate molecular properties by revealing subtle changes in electronic environments, molecular dynamics and molecular conformations.[4,5]

Brooker's merocyanine (BM),[6] is a highly conjugated dye known for its strong solvatochromic behaviour, namely, its colour changes depending on the solvent polarity (Fig. 1A). Numerous seminal studies have established the theoretical and experimental foundations of solvatochromism, including key reports on spectroscopic correlations—particularly between UV/Vis and NMR spectroscopy.[7–14]

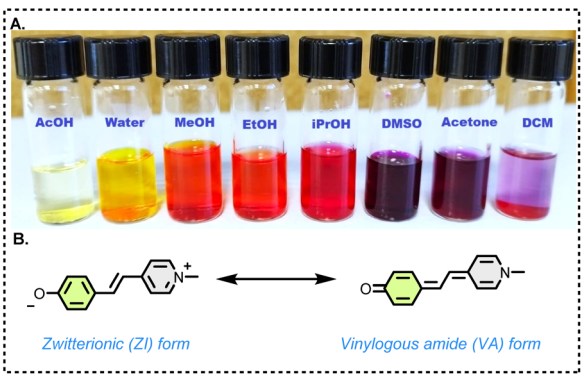

Fig. 1 (A) BM in solution in various solvents. (B) The structural formula of BM.

The unique electronic structure of BM makes it valuable in developing advanced materials for sensors, photonic devices, and molecular electronics.[15,16] Its well-defined electronic transitions and ability to exist in multiple resonance forms make BM an ideal model for exploring fundamental mechanisms of nonlinear optical behaviour, such as intramolecular charge transfer and polarizability, which are central to the development of advanced photonic and optoelectronic materials.[17–19]

Structurally, BM, **1a** can be drawn in two canonical forms, as shown in Fig. 1B. The form on the left preserves the aromaticity of the two rings, and is zwitterionic, involving charge separation, and would, therefore, be expected to be dominant in polar solvents. Conversely, the form on the right is a vinylogous amide and is neutral, eliminating the charges on the heteroatoms expected to be dominant in non-polar solvents.

In our previous work on the synthesis and applications of BM derivatives,[20,21] we observed substantial solvent-dependent variations in their NMR spectra of various derivatives of BM's consistent with literature reports.[22,23]

This is reminiscent of the well-known solvatochromic material, Reichardt's dye, from which C. Reichardt derived the UV/Vis-based $E_T(30)$ index of solvent polarity (Reichardt himself mentions Brooker as an early proposer of a dye-based scale of solvent polarity).[24] Extending this concept further, Frimer *et al.* reported an NMR study of Reichardt's dye, in which they showed that ^{13}C chemical shifts correlate very well with solvent polarity and, therefore, with colour.[25]

Although basic NMR study of BM laid the foundation, here we significantly expand this scope by systematically investigating the correlation of $E_T(30)$ index and the photophysical properties of nine BM derivatives. Our results reveal a direct correlation between solvent polarity and both NMR chemical shifts (^1H, ^{13}C and ^{15}N) and UV-Vis absorption, demonstrating that changes in the local environment are consistently reflected in both spectroscopic signatures. These findings provide new insights into the structure–property relationships in BM dyes and underscore the broader applicability of NMR and UV-Vis

[a]*Department of Chemistry, Bar-Ilan University, Ramat-Gan, 52900, Israel. E-mail: abed.saady@biu.ac.il*

[b]*Schulich Faculty of Chemistry, Technion-Israel Institute of Technology, Haifa City 3200003, Israel*

† Electronic supplementary information (ESI) available. See DOI: https://doi.org/10.1039/d5ra03758a

methods for understanding solvatochromism in this important class of materials.

Results and discussion

Compounds **1a–i**, **2g** and **2i** (Fig. 2) were synthesized according to a previously reported procedure.[20,21]

The UV/Vis spectrum of parent merocyanine **1a** shows two absorption maxima, one in the yellow (λ_{max} = *ca.* 600 nm), and one in the violet region (λ_{max} = *ca.* 400 nm) of the spectrum. We measured UV/Vis spectra for **1a** in a variety of solvents ranging from THF (least polar) to water (most polar) (see; ESI†).

A plot of the wavelengths of the absorption maxima in nm and eV, as a function of the $E_T(30)$ index of the polarity of the solvent is shown in Fig. 3. As can be seen, there is a good correlation between $E_T(30)$ and the λ_{max} values, which suggests that the ability of the solvents to induce separation of charges is similar for both the Brooker and the Reichardt dyes.

With a view to compare the UV/Vis and NMR spectral properties we then took ^{1}H and ^{13}C NMR spectra of **1a** in a variety of solvents. We unambiguously assigned all the NMR signals by using several 2D-NMR techniques (COSY – ^{1}H × ^{1}H correlation, HMQC – ^{1}H × ^{13}C one-bond correlation and HMBC – ^{1}H × ^{13}C long-range correlation). In addition, we indirectly obtained ^{15}N chemical shifts by ^{1}H × ^{15}N HMBC spectra (see; ESI, Table S1†).

As the polarity increases, the high-wavelength peak becomes less intense and approaches the lower wavelength, and for the most polar solvents (methanol and water) it cannot be observed. (Full data in the ESI, Table S12†).

Inspection of the data indicates the chemical shifts of carbons 5, 7 and 10 are the most solvent-dependent – (Fig. 4). C-10 is deshielded in non-polar solvents, suggesting a more carbonyl-like nature, and shielded in polar solvents – more resembling an aromatic-carbon. Following this trend, even numbered carbons (C-8, C-6), also have negative slopes (albeit smaller in absolute terms) in the $\delta \times E_T(30)$ graph. Conversely, odd-number carbons (C-3, C-5, C-7) have positive slopes. Especially striking are the chemical shift of the N-1 nitrogen, with a strongly positive slope (Fig. 4). In non-polar solvents, this nitrogen is more like a VA and therefore deshielded relative to polar solvents, where it is more resembles a typical pyridinium salt.

All the compounds examined dissolve well in CD_3OD and DMSO-D_6; however, compounds **1a–i**, **2g** and **2i** can be dissolved in less polar solvents (*e.g.* $CDCl_3$) or in D_2O, but this often resulted in more dilute samples which required overnight runs. Also, methanol and DMSO are representative more and less polar solvents, [$E_T(30)$ = 55.5 and 45.1, respectively].

Therefore, for the sake of brevity and comparison purposes, we decided to consistently report in the body of this paper only

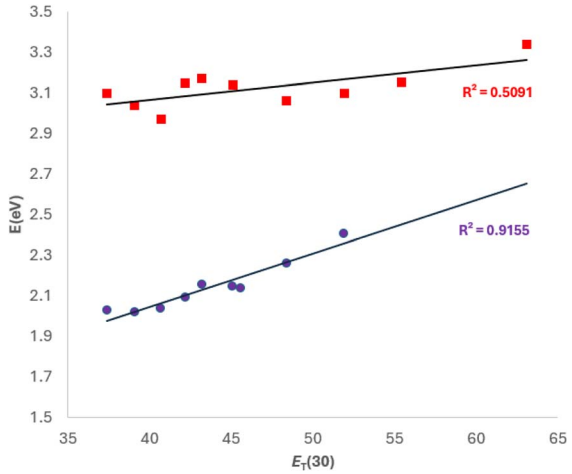

Fig. 3 λ_{max} (eV) values for **1a**, as a function of the polarity of the solvent [$E_T(30)$ values, in kcal mol^{-1}] ranging from THF (least polar) to water (most polar).

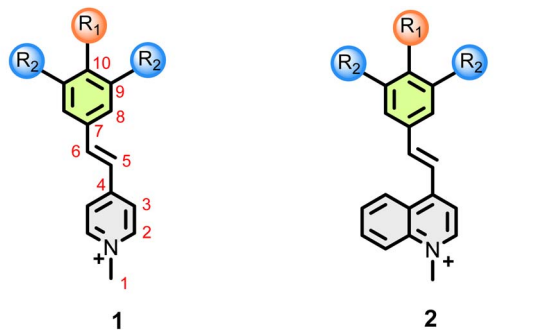

a. R_1 = O$^-$, R_2 = H
b. R_1 = H, R_2 = H
c. R_1 = OCH_3, R_2 = H
d. R_1 = NH_2, R_2 = H
e. R_1 = $N(CH_3)_2$, R_2 = H
f. R_1 = $NHCOCH_3$, R_2 = H
g. R_1 = OH, R_2 = H
h. R_1 = O$^-$, R_2 = F
i. R_1 = OH, R_2 = F

Fig. 2 BM derivatives synthesized and evaluated in this study.

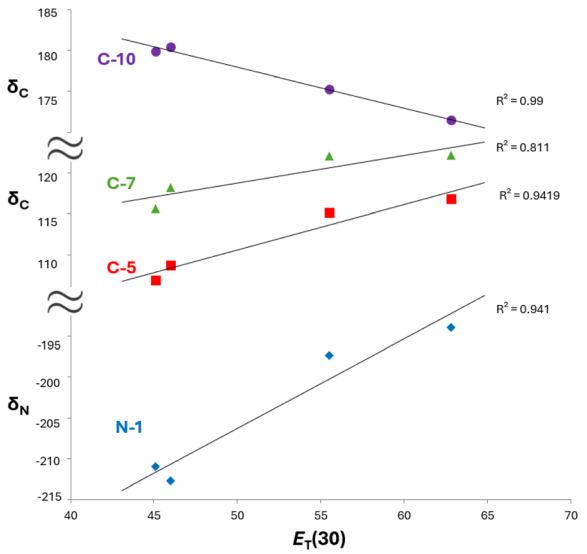

Fig. 4 Solvent dependence of the chemical shifts for selected carbon and nitrogen atoms of **1a**.

the differences of the chemical shifts in these two solvents of ($\delta_{methanol} - \delta_{DMSO}$) for carbons 5, 7 and 10 and for N-1 (Table 1).

The complete data we have obtained is available in the ESI.†

Unsurprisingly, compound **1b** is not solvatochromic – all solutions we examined were orange, this finding is expected, as no zwitterionic canonical form can exist. The observed uniformity of the UV/Vis spectra is mirrored in the NMR results – much smaller absolute $\delta_{methanol} - \delta_{DMSO}$ values are observed (Table 1).

Compounds **1b**, was analysed by single crystal X-ray diffraction (Fig. 5).

Similarly, dyes **1c–1f** are also not solvatochromic, as seen both by the consistent orange colour of their solutions as by their small absolute $\delta_{methanol} - \delta_{DMSO}$ values (Table 1), as compared to **1a**. It turns out that, for all compounds **1b–1f**, *for each specific* carbon/nitrogen atom the $\Delta\delta$ values are not zero but are very similar (if not quite identical) across the sequence of dyes, and are likely due to unrelated specific solvent interactions – and we can use these trends as a baseline to distinguish other, more subtle changes, as will be shown below.

Interestingly, **1g** is the protonated (phenol rather than phenolate) form of **1a** – and, unlike **1b–1f**, it was found to be solvatochromic. Solutions of **1g** show the characteristic colour change of phenolate **1a** (red in methanol, purple in DMSO, Fig. 1A) – even though to obtain a vinylogous amide form a carbonyl oxygen would have to carry a positive charge and would likely deprotonate, with the departing H^+ attaching itself either to the nitrogen or to a solvent molecule.

In either case, we could envisage an equilibrium between an acid and its conjugate base or between tautomers, but not a resonance hybrid. Inspection of the $\Delta\delta$ data as indicated in Table 1, indeed suggests an equilibrium of this type. $\Delta\delta$ values may be used to estimate the degree of deprotonation for the phenol – specifically, the $\Delta\delta$ value ($\delta_{methanol} - \delta_{DMSO}$) for N-1 is +13.7 for the phenolate, but *ca.* −2 for the non-solvatochromic substances (**1b–1f**); this means the corrected $\Delta\delta$ for the nitrogen atom is *ca.* +16 ppm.

For phenol **1g**, the corrected $\Delta\delta$ would be *ca.* +3 ppm, indicating *ca.* 20% deprotonation to the phenolate **1a**. This is supported by the observation of small broadenings of some carbon signals (in DMSO, 20 and 7 Hz for C-5 and C-7, respectively), indicating that there is an equilibrium which, at 300 K, is not fast enough for the extreme narrowing of the lines. It is worthwhile noticing that in **1d** and **1f**, we see no indication of an equivalent deprotonation of a less acidic NH-containing substituent.

Compound **2g** is related to **1g**, having a quinoline system rather than pyridine. The behaviour of the two phenols is very similar – **2g** is also solvatochromic, and the $\Delta\delta$ values in this

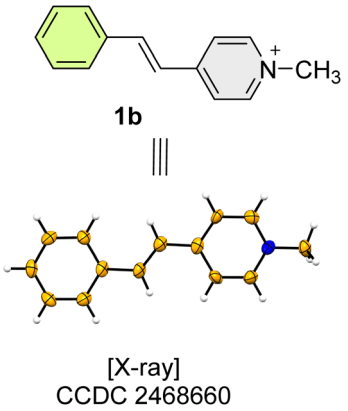

Fig. 5 Solid-state structure of **1b**, shown in ORTEP mode. Ellipsoids are shown at 50% probability.

Table 1 indicate that also in this case, the OH group is partially deprotonated. The degree of deprotonation for this phenol, estimated as in item 2.4, indicates an even larger value – *ca.* 50%.

Compounds **1h** and **1i** are the phenolate/phenol pair, having difluoro substitution *ortho* to the OH group.[26] As expected, **1h** is indeed solvatochromic and the NMR data (ESI, Table S2†) clearly indicates the contribution of the vinylogous amide form as in the parent **1a**. To our surprise, phenol **1h**, however, does not deprotonate and is not solvatochromic, even though the *ortho* fluorine substituents are expected to increase the acidity of the phenol function.

Compound **2i** is the quinoline version of the *ortho*-difluorinated phenol. **2i**, however, is solvatochromic and is >80% deprotonated in solution (ESI, Table S9†). An equilibrium between protonated and deprotonated forms is also indicated by extensive broadening (the kinetics of this process seem to be slightly slower than what we observed for **1g**) of several of the NMR lines (see ESI† file) – the broadest carbon signal (linewidth *ca.* 40 Hz) is C-10.

In order to estimate the contribution of the VA canonical form to the structure of **1a**, we used ^{15}N chemical shifts as the most sensitive tool for this purpose. We thus measured the NMR spectra for 1,4-dimethylpyridinium iodide, **3**, and 1-methyl-4(1*H*)-pyridinone, **4**, as model compounds (Fig. 6).

These compounds were selected as reference structures for the two principal resonance forms of BM: **3** as a representative of the charge-separated pyridinium form, and **4** as a model for the vinylogous amide form. This allows a direct comparison of ^{15}N chemical shifts, facilitating a quantitative assessment of resonance contributions in the studied dyes.

Table 1 $\delta_{methanol} - \delta_{DMSO}$ for selected nuclei

	1a	1b	1c	1d	1e	1f	1g	2g	1h	1i	2i
C-5	8.24	0.71	0.72	1.44	0.75	1.24	2.57	3.81	6.09	0.61	6.00
C-7	6.41	1.53	1.56	2.72	1.83	2.40	3.46	2.09	8.45	2.36	6.25
C-10	−4.58	1.48	2.47	1.55	2.27	1.25	−0.04	−1.76	−4.20	2.19	−4.84
N-1	13.7	−1.9	−2.2	−1.8	−2.6	−1.5	0.8	6.4	6.6	−1.8	12.1

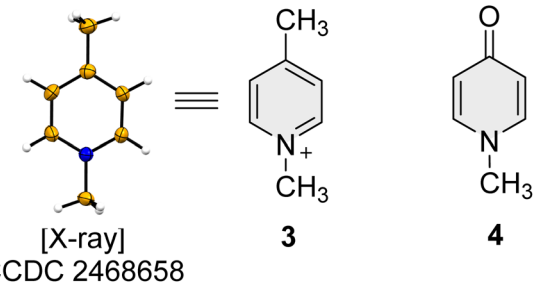

Fig. 6 Structure of model compounds **3** and **4** and solid-state structure of **3**, shown in ORTEP mode. Ellipsoids are shown at 50% probability.

The ^{15}N chemical shift for salt **3** is indeed quite solvent-independent, at *ca.* −183 ppm, and this value is a good reference for this type of quaternary nitrogen atom. Conversely, we use the ^{15}N chemical shift – *ca.* −246 ppm – of **4**, in $CDCl_3$, as a model for the uncharged, vinylogous amide form. This chemical shift is quite typical for amide nitrogen.

We thus get a $\Delta\delta$ value of 63 ppm between the two chemical shifts, which allows us to estimate the contribution of the VA form of **1a** as 44% in DMSO, 22% in methanol and 17% in water. Compound **4** can be also described as a resonance hybrid between the vinylogous amide form shown here and a charge-separated zwitterion. Using the same $\Delta\delta$ value, we estimate that the canonical form depicted in **4** is the dominant contributor to the resonance hybrid (78%) even in methanol. Of course, in all amides there is *some* contribution of a charge-separated (zwitterionic) form, and this is especially true for a vinylogous amide, even in a non-polar solvent, so that these values are obviously overestimates, but we still feel that they add to our understanding of this type of chemical function.

Conclusions

In conclusion, we have demonstrated that solvent polarity and molecular structure play key roles in dictating the electronic properties and resonance equilibria of merocyanine dyes. Our combined UV/Vis and NMR studies reveal that only dyes capable of adopting zwitterionic resonance forms, such as **1a**, exhibit strong solvatochromism, with both absorption maxima and NMR chemical shifts shifting systematically with solvent environment. Through analysis of structural analogues and ^{15}N chemical shifts, we show that substituents finely tune the extent of charge separation and deprotonation equilibria. These findings provide a clear framework for designing merocyanine-based dyes and probes with tailored, environment-sensitive properties.

Experimental

General information

Reagents and solvents were purchased from commercial sources and were used without further purification. Progress of reactions was monitored by TLC on precoated Merck silica gel plates (60F-254), with visualization by UV light. Compounds were characterized by nuclear magnetic resonance using a Bruker Avance-III-700 spectrometer (700.45, 176.13 and 70.98 MHz for ^{1}H, ^{13}C and ^{15}N, respectively). Chemical shifts are reported in ppm units (δ) relative to TMS (δ_H and $\delta_C = 0$ ppm). The residual signals of under-deuterated solvents ($\delta_H = 7.26$ ppm in $CDCl_3$, 4.79 ppm in D_2O and 2.50 ppm in $(CD_3)_2SO$) in ^{1}H NMR spectra, and the central peaks of $CDCl_3$ ($\delta_C = 77.00$ ppm), $(CD_3)_2SO$ ($\delta_C = 39.52$ ppm) or TMS in ^{13}C NMR spectra were used as internal standards. The coupling constants (J), calculated according to the first order NMR spectra, are reported in Hz. Standard abbreviations indicating multiplicity were used as follows: m = multiplet, quint = quintet, q = quartet, t = triplet, d = doublet, s = singlet, br = broad, sept = septet. ^{1}H signal assignment was carried out using 2D NMR methods (COSY, HMQC, HMBC) as appropriate. Chemical shifts for ^{15}N NMR spectra were referenced to neat nitromethane (an external standard). Absorption spectra were measured on a UV-2401PC UV-VIS recording spectrophotometer (Shimadzu, Kyoto, Japan).

Compounds **1a–1i**, **2g** and **2i** were synthetized according to literature procedures.[20,21] Typically, 1,4-dimethylpyridinium iodide, **3** (0.1 mmol), the appropriate substituted benzaldehyde (0.1 mmol), and a catalytic amount of piperidine were dissolved in 2 mL of absolute ethanol in a 10 mL microwave CEM vial. The reaction mixture was irradiated in a microwave reactor at 80 °C for 2 hours. After cooling to room temperature, 10 mL of diethyl ether was added to precipitate the product, which was collected by vacuum filtration and washed three times with 3 mL portions of diethyl ether to afford the pure compound. The products were characterized by NMR and UV/Vis spectroscopy (see ESI† for details).

Data availability

The data supporting this article have been included as part of the Electronic supplementary information (ESI): Detailed spectroscopic data; NMR, UV/Vis spectra and SCXRD as appropriate of the reported compounds. CCDC 2468658 and 2468660. For ESI and crystallographic data in CIF or other electronic format see DOI: **https://doi.org/10.1039/d5ra03758a**

Author contributions

The manuscript was written through contributions of all authors. All authors have given approval to the final version of the manuscript.

Conflicts of interest

There are no conflicts to declare.

Acknowledgements

Abed Saady thanks Bar-Ilan University (Start-up grant) and the Council for Higher Education (MAOF scholarship).

Notes and references

1 Y. Hu, K. Cheng, L. He, X. Zhang, B. Jiang, L. Jiang, C. Li, G. Wang, Y. Yang and M. Liu, *Anal. Chem.*, 2021, **93**, 1866–1879.
2 S. W. Homans, *Angew. Chem., Int. Ed. Engl.*, 2004, **43**, 290–300.
3 H. Zhu and L. A. O'Dell, *Commun. Chem.*, 2021, **57**, 5609–5625.
4 E. E. Kwan and S. G. Huang, *Eur. J. Org Chem.*, 2008, **2008**, 2671–2688.
5 T. D. Claridge, *High-resolution NMR Techniques in Organic Chemistry*, Elsevier, 2016.
6 L. Brooker, G. Keyes and D. Heseltine, *J. Am. Chem. Soc.*, 1951, **73**, 5350–5356.
7 N. K. Karmakar, S. Pandey, R. K. Pandey and S. S. Shukla, *Appl. Spectrosc. Rev.*, 2021, **56**, 513–529.
8 N. Boens, L. Wang, V. Leen, P. Yuan, B. Verbelen, W. Dehaen, M. Van der Auweraer, W. D. De Borggraeve, L. Van Meervelt and J. Jacobs, *J. Phys. Chem. A*, 2014, **118**, 1576–1594.
9 D. Avcı, Ö. Tamer and Y. Atalay, *J. Mol. Liq.*, 2016, **220**, 495–503.
10 W. Kuznik, M. N. Kopylovich, G. I. Amanullayeva, A. J. Pombeiro, A. H. Reshak, K. T. Mahmudov and I. Kityk, *J. Mol. Liq.*, 2012, **171**, 11–15.
11 J. M. Marković, N. P. Trišović, D. Mutavdžić, K. Radotić, I. O. Juranić, B. J. Drakulić and A. D. Marinković, *Spectrochim. Acta Mol. Biomol. Spectrosc.*, 2015, **135**, 435–446.
12 A. V. Kulinich, N. A. Derevyanko and A. A. Ishchenko, *J. Photochem. Photobiol., A*, 2007, **188**, 207–217.
13 D. Avcı, S. Altürk, Ö. Tamer, M. Kuşbazoğlu and Y. Atalay, *J. Mol. Struct.*, 2017, **1143**, 116–126.
14 L. Zhang, J. M. Cole and X. Liu, *J. Phys. Chem. C*, 2013, **117**, 26316–26323.
15 L. G. Nandi, C. R. Nicoleti, I. C. Bellettini and V. G. Machado, *Anal. Chem.*, 2014, **86**, 4653–4656.
16 J. Nicolini, F. M. Testoni, S. M. Schuhmacher and V. G. Machado, *Tetrahedron Lett.*, 2007, **48**, 3467–3470.
17 M. Dekhtyar, W. Rettig, A. Rothe, V. Kurdyukov and A. Tolmachev, *J. Phys. Chem. A*, 2019, **123**, 2694–2708.
18 V. Cavalli, D. C. da Silva, C. Machado, V. G. Machado and V. Soldi, *J. Fluoresc.*, 2006, **16**, 77–86.
19 H. Mustroph, *Phys. Sci. Rev.*, 2022, **7**, 143–158.
20 A. Saady, E. Varon, A. Jacob, Y. Shav-Tal and B. Fischer, *Dyes Pigm.*, 2020, **174**, 107986.
21 A. Saady, P. Sudhakar, M. Nassir and A. Gedanken, *Ultrason. Sonochem.*, 2020, **67**, 105182.
22 J. O. Morley, R. M. Morley, R. Docherty and M. H. Charlton, *Am. Chem. Soc.*, 1997, **119**, 10192–10202.
23 J. O. Morley, R. M. Morley and A. L. Fitton, *Am. Chem. Soc.*, 1998, **120**, 11479–11488.
24 C. Reichardt, *Chem. Rev.*, 1994, **94**, 2319–2358.
25 M. Afri, H. E. Gottlieb and A. A. Frimer, *Can. J. Chem.*, 2014, **92**, 128–134.
26 Compound **1h** was obtained after treatment of compound **1i** with aqueous KOH according to the general protocol appears on ref. 6.